Vibrational Mean Free Paths and Thermal Conductivity Accumulation Functions for Amorphous Materials

Jason M. Larkin[1] and Alan J. H. McGaughey[1]

[1]*Department of Mechanical Engineering*

Carnegie Mellon University

Pittsburgh, PA 15213

(Dated: June 25, 2013)

Abstract

BEGINALAN

Understanding thermal transport in crystalline systems requires detailed knowledge of phonons, which are the quanta of energy associated with atomic vibrations. By definition, phonons are non-localized vibrations that transport energy over distances much larger than the atomic spacing. For disordered materials (e.g., alloys, amorphous phases), with the exception of very long-wavelength (low-frequency) modes, the vibrational modes are localized and do not propagate like phonons. The film thickness and temperature dependence of thermal conductivity measured by experiments show indirectly that propagating modes contribute significantly for a-Si but not a-SiO2, with contribution from vibrational modes with large mean free paths (100-1000 nm). Recent measurements using a broadband FDTR technique argue that these vibrational mean free paths can be probed by varying the penetration depth to measure the thermal conductivity accumulation function. Using lattice dynamics calculations and molecular dynamics simulations on realistic models of a-SiO2 and a-Si, we predict and characterize the contributions from phonons and localized vibrations to vibrational thermal conductivity. The vibrational mean free paths are predicted for these two amorphous materials and the thermal conductivity accumulation function is compared with experimental results, particularly from Regner et al.

ENDALAN

I. INTRODUCTION

BEGINALAN

Amorphous silicon (a-Si) and nanocrystalline silicon have applications in high-efficiency solar cells.(cite) Films and substrates made of a-SiO2 and a-Si have wide application. (cite) Understanding the thermal transport in these amorphous systems is critical to improving their performance. Thermal transport at scales comparable to phonon wave- lengths and mean free paths (MFPs) is presently a topic of considerable interest.[1–4] Recently, nanostructured materials such as nanowires, superlattices, and composites with strongly reduced thermal conductivities due to phonon scattering at interfaces and boundaries have been reported and are being considered for use in thermoelectric applications.[3–6] Recent empirical and first-principles calculations show that MFPs of phonons relevant to thermal conductivity vary by more than 5 orders of magnitude in crystalline materials.[7] Traditionally, empirical expressions and simple relaxation time models have been the only means to estimate MFPs.[8]

Experimentally, inelastic neutron scattering has been used to measure phonon lifetimes in certain materials, but this technique is more suited for single crystal samples.[9] Koh et al. proposed a time-domain thermal reflectance (TDTR) technique which uses a variation of modulation frequency to measure MFPs, but this technique is limited by the modulation frequency.[10] An x-ray diffraction and thermoreflectance technique can measure ballistic transport in some structures.[11] The thermal conductivity accumulation function can be predicted for bulk crystalline systems using TDTR and frequency-domain thermal reflectance (FDTR) techniques. (cite) The understanding of the accumulation function for bulk crystalline is understood fairly well experimentally[12] and theoretically.[13] However, understanding of the accumulation in amorphous systems is still not well understood.[14–19] Recent measurements by Regner using broadband FDTR argue that the thermal conductivity accumulation function can be measured by varying the penetration depth of the experimental measurement.[20]

Experimental measurements of the thermal conductivity of thin films of a-SiO2 and a-Si at varying temperatures gives indirect information about the low-frequency, propagating modes.(cite) For a-SiO2, varying temperature and film thickness[21,22] measurements all suggest that the propagating modes contribute a negligible amount to thermal conductivity.

However, the behavior of the low-frequency modes has only recently been understood by experimental measurements,[23–27] where a cross-over of the low-frequency scaling of the vibrational lifetimes from Rayleigh (quartic)(cite) to Umklapp (quadratic)(cite) is observed.

For a-Si the low-frequency behavior is less understood. Temperature varying(cite) and film thickness-varying measurements[15,17,18,28–32] suggest multiple and different behavior of the low-frequency scaling of the mean free paths of vibrational modes in a-Si. Comparison of experimental measurements by Pompe[33] and Cahill[15,34] show a plateau of thermal conductivity with temperature, which can be predicted by the the model from FKAW which assumes a ω^{-4} scaling.[14] Low temperature conductivity and specific heat measurements demonstrate that the propagating modes in a-Si and doped a-Si follow $\Lambda \propto \omega^{-2}$,[30,35] where no thermal conductivity plateau is observed[18,30,35] There is a clear film thickness t_f dependence of the thermal conductivity of a-Si, particularly for $t_f > 10$ μm, (cite) where conductivities of $1.4 - 6$ W/m-K have been reported. (cite) Both quadratic[16] and quartic[14,18**?**] scalings of the low-frequency MFPs have been considered to explain these experimental measurements. More experimental measurements are needed to understand the low-frequency behavior in a-Si thin films.(cite)

Low temperature conductivity and specific heat measurements demonstrate that the propagating modes in a-Si and doped a-Si follow $\Lambda \propto \omega^{-2}$.[30,35] Comparison of experimental measurements by Pompe[33] and Cahill[15,34] show a plateau of thermal conductivity with temperature, which can be predicted by the the theory from FKAW which assumes a ω^{-4} scaling.[14] Zink et al. measured the thermal conductivity of e-beam evaporated amorphous silicon thin films over a wide tem- perature range and found now plateau, which is predicted from the FAB theory and an ω^{-2} scaling.[16]

In this work, we perform Molecular Dynamics (MD) simulations and Lattice Dynamics calculations on large models of a-SiO2 and a-Si. The results are used to understand recent experimental measurements using a broadband frequency domain thermal reflectance (FDTR) technique with varying penetration depths L_p.[20] Large MD simulations of models for a-SiO2 show (within the errors) no dependence on the system size, indicating that propagating modes do not make a significant contribution to thermal conductivity. This is confirmed by modal analysis, which demonstrates that propagating modes contribute a negligible amount to thermal conductivity. At low frequency, a quadratic scaling of the vibrational mode lifetimes is a reasonable fit to the predictions, in agreement with previous

models of a-SiO2.(cite)

We predict the thermal conductivity of bulk a-Si using (to our knowledge) the largest MD simulation for a model of a-Si.(cite) Scaling of thermal conductivity with system size indicates that the low-frequency propagating modes in bulk a-Si follow a Debye-like model with a quadratic scaling of the mode lifetime with frequency. (cite) A modal analysis of a large a-Si model supports the evidence for quadratic scaling of lifetimes at low frequency, which is not definitive using the AF diffuson theory.[14,16] The propagating modes are found to contribute significantly to the thermal conductivity of a-Si an amount similar to that predicted by other models of a-Si.(cite)

The spectrum of vibrational MFPs and the accumulated thermal conductivity (cite) are predicted for a-SiO2 and a-Si. The thermal conductivity for our model of a-SiO2 accumulates within 95% of its bulk value for vibrational mean free paths (MFPs) < 10 nm. This result explains the experimental measurements of Regner et al, which show no measured dependence of the thermal conductivity on L_p,[20] and experimental measurements of the thermal conductivity of thin films which show no dependence on film thickness.(cite)

Using a simple boundary scattering model, the accumulated thermal conductivity of a-Si thin films are predicted from our model of bulk a-Si. The predicted accumulated thermal conductivity reproduces the experimentally measured penetration depth-dependent thermal conductivity qualitatively.(cite) We consider both quadratic and quartic scalings of the low-frequency vibrational lifetimes. By considering both scalings, our model of thin-film a-Si thermal conductivity accumulation can span the range of the lower(cite) and higher[17,18] experimentally measured thermal conductivity of varying thickness a-Si thin films.

The predicted contribution to thermal conductivity of non-propagating modes from our model of a-Si is in good agreement with the plateau of accumulated thermal conductivity from broadband FTDR. The quadratic scaling of low-frequency mode lifetimes does not predict the steep dependence of thermal conductivity on L_p, while the quartic scaling can qualitatively. Given the lack of experimental measurements of the low-frequency scaling of vibrational mode lifetimes,(cite) low-temperature broadband FDTR measurements can help to show which scaling, quadratic or quartic, is present in a-Si thin films with varying deposition technique. The results could answer the question of whether quartic versus quadratic scaling is responsible for the large thickness variation of the thermal conductivity of a-Si thin films.

ENDALAN

II. THEORETICAL FORMULATION

A. Vibrational Thermal Conductivity

BEGINALAN

To calculate the total vibrational thermal conductivity k_{vib} of amorphous solids, we predict the contributions from k_{ph} and k_{AF},

$$k_{vib} = k_{ph} + k_{AF}, \tag{1}$$

where k_{ph}[36–38] is the contribution from phonons or phonon-like modes and k_{AF} is the contribution from the Allen-Feldman (AF) theory of diffusons.[14] The form of Eq. (1) has been used in several previous studies with varying assumptions. The various assumptions all lead to predictions that k_{ph} is a significant fraction($> 20\%$) of k_{vib}.(cite)

We predict the contribution k_{ph} using a Debye-like model,

$$k_{ph} = \frac{1}{V}\int_0^{\omega_{cut}} d\omega DOS(\omega)C(\omega)D(\omega), \tag{2}$$

and the diffuson contribution k_{AF} using[14,16]

$$k_{AF} = \frac{1}{V}\sum_{\omega_i > \omega_{cut}} C_i(\omega)D_{AF,i}(\omega) \tag{3}$$

The phonon contribution k_{ph} is written as an integral because the finite simulation sizes studied in this work (and others)[14,16] limit the lowest frequency vibrational modes which can be studied. The diffuson contribution k_{AF} is written as a sum because there are enough high-frequency diffuson modes in the finite-size systems studied.[14,16] The cut-off frequency ω_{cut} identifies the transition from phonon-like to diffuson modes.[14–18]

Phonon-like behavior can be identified for a-Si in this work and others, both experimentally[12,17,18,20] and numerically.[14,16,39,40] Including the phonon-like contribution k_{ph} for a-Si is not qualitatively sensitive to the choice of model[14,16,17] or ω_{cut}.[14,16–18,41]

In this work, we identify the phonon limit by ω_{cut} in Eq. (1), in Section IV D. By identifying ω_{cut} the contribution of phonon-like modes in a-Si and a-SiO_2 is quantified in Section V A and the thermal conductivity accumulation is predicted in Section V B.

ENDALAN

B. Phonons

BEGINALAN

Eq. 2 can be derived starting with the Kubo theory,[18,24,42–44] which is used to derive the Allen-Feldman diffuson theory,**??** and taking the limit of zero phonon self-energy.[24] Eq. (2) can also be obtained using the single-mode relaxation time approximation to solve the Boltzmann transport equation.[38] Assumed in Eq. (2) are isotropy (valid for an amorphous material) and a single phonon polarization,(cite) making the properties a function of the mode frequency ω only. The choice of a single phonon polarization (i.e., an averaging of the transverse and longitudinal branches)(cite) does not significantly change the results predicted in this work or others.[14–18,24]

For a phonon gas, Eq. (2) has mode diffusivity

$$D(\omega) = \frac{1}{3} v_g^2(\omega)\tau(\omega). \tag{4}$$

The physical picture is of propagating plane waves which travel with velocity v_g for a time τ before scattering. An equivalent physical picture in terms of a scattering length is

$$D(\omega) = \frac{1}{3} v_g(\omega)\Lambda(\omega), \tag{5}$$

where Λ is the phonon mean free path (MFP), defined as

$$\Lambda(\omega) = v_g(\omega)\tau(\omega). \tag{6}$$

Both Eqs. (4) and (5) are valid in the propagating limit, i.e. the Ioffe-Regel (IR) limit.(cite)

In disordered system, Eqs. and are only valid in the low-frequency, long-wavelength limit.(cite) Because of this, we focus on the mode diffusivity D as the fundamental quantity. The phonon thermal diffusivity, $D_{ph}(\omega)$, is modeled using

$$D_{ph}(\omega) = B\omega^{-2} \tag{7}$$

which is a scaling predicted for Umklapp phonon-phonon scattering, (cite callaway) and

$$D_{ph}(\omega) = B\omega^{-4} \tag{8}$$

which is the scaling predicted by Rayleigh scattering.[45] Both scalings Eqs. and also assume

Since we use MD simulations, which are classical and obey Maxwell-Boltzmann statistics,[46] we take the phonon and diffuson specific heat to be $C(\omega) = C(\omega_i) = \frac{k_B}{V}$ in the harmonic limit, where V is the system volume. This harmonic approximation has been shown to be valid for a-Si modeled using the Stillinger-Weber potential at the temperatures of interest here.(cite) Taking the classical limit for the specific heat allows for a direct comparison between the MD- and lattice dynamics-based methods.

Under the Debye approximation, which assumes isotropic and linear dispersion (i.e., $v_g = v_s$), the density of states, $DOS(\omega)$, is

$$DOS(\omega) = \frac{3\pi\omega^2}{2v_{s,DOS}^3}, \tag{9}$$

where v_s is an appropriate sound speed.(cite)

The form for $D(\omega)$ (Eq. (7)) and the $DOS(\omega)$ (Eq. (9)) cause a cancellation of ω dependence in Eq. (2) and ensures that the thermal conductivity is finite. The form for $D(\omega)$ (Eq. (8)) causes the thermal conductivity (Eq. (2)) to diverge in the low-frequency limit as the system size is increased as $L^{1/4}$.(cite)

ENDALAN

While the classic limit for the mode specific heat is an over-prediction for the high frequency modes in a-Si, the non-propagating contribution predicted by broadband FTDR matches the prediction from the AF diffuson theory. Adjusting the specific heats to include quantum statistical effects...

We can thus focus on the less understood low-frequency propagating contribution.

Because we use molecular dynamics (MD) simulations, we

In general, the thermal conductivity k_{ph} and group velocity v_g depend on the spatial direction $\mathbf{n}$. Since the amorphous materials studied in this work are isotropic, k_{ph} and v_g are scalar quantities independent of the direction $\mathbf{n}$.

C. Diffusons

BEGINALAN

For disordered systems, the vibrational modes are no longer pure plane-waves (i.e., phonon modes), except in the low-frequency (long-wavelength) limit.(cite) When applied in the classical limit, the Allen-Feldman (AF) theory computes the contribution of diffusive,

non-propagating modes (i.e., diffusons) to thermal conductivity[43]

$$D_{AF,i} = \frac{\pi V^2}{\hbar^2 \omega_i^2} \sum_{j \neq i} |\langle i|J_{x,y,z}|j\rangle|^2 \delta(\omega_i - \omega_j) \tag{10}$$

where $D_{AF,i}$ is the mode diffusivity and ω_i is the frequency of the ith diffuson. The diffusivity of diffusons can be calculated from harmonic lattice dynamics theory.[14,16,43]

ENDALAN

D. Thermal Diffusivity and Conductivity Limits

BEGINALAN

The relative contribution of k_{ph} and k_{AF} to k_{vib} has been estimated to be approximately equal for a model of a-Si at 300 K,[40] while earlier studies find that k_{ph} is less than half.[14,16] Assuming a constant contribution k_{AF} 1 W/m-K, experimental measurements and estimates show that the contribution from k_{ph} is low as 20%,[15,16] 40%,[17] and as high as,[18] all depending on the assumed scaling of the low-frequency vibrational scattering. The thermal conductivity k_{vib} has also been estimated for a-GeTe[47], where $_{ph} \approx 0$ and $k_{vib} \approx k_{AF}$, and silicon nanowires,[41] where $k_{ph} \approx k_{AF}$.

For disordered materials In the low-frequency, long-wavelength limit, the mode thermal diffusivity has the form of Eq. (7) or (8).(cite) The mode diffusivities generally decrease with increasing frequency,(cite) often reaching a plateau,(cite) and then decrease exponentially to zero as the modes become localized.(cite) Diffuson thermal diffusivities, Eq. (10), cannot in general be expressed as either Eq. (4) or (5). For disordered systems, the mode group velocities, lifetimes, MFPs cannot be estimated independently.[14,16,43,48,49]

It is useful to consider a high-scatter limit for the mode diffusivity,

$$D_{HS} = \frac{1}{3} v_s a, \tag{11}$$

where it is assumed that all vibrational modes travel with the sound speed, v_s, and scatter over a distance of the lattice constant, a. This diffusivity assumption leads to a high-scatter (HS) limit of thermal conductivity in the classical limit[50]

$$k_{HS} = \frac{k_{\mathrm{B}}}{V_b} b v_s a, \tag{12}$$

where V_b is the volume of the unit cell and b is the number of atoms in the unit cell.

For amorphous systems, the spatial disorder creates strong scattering, and k_{vib} tends to be near the high-scatter limit k_{HS}.(cite) It was demonstrated by Kittel that the thermal conductivity of glasses above 20 K could be interpreted using a temperature-independent high-scatter diffusivity on the order of Eq. (11). Since this corresponds to a phonon model with MFP $\Lambda = a$, too small to justify use of the model, implies that the dominant modes in most glasses are diffusons and not phonons.(cite)

One way to interpret this result is to use assume $k_{vib} = k_{AF} = k_{HS}$. Amorphous Lennard-Jones argon is dominated by high-scatter modes,[49] as is a model of a-GeTe, and both their $k_{vib} \approx k_{HS}$.[47] For a-SiO_2, $k_{vib} \approx 2k_{HS}$, while it is unclear what the appropriate lattice constant a should be.(cite) For a-Si, the experimentally measured thermal conductivity at 300 K $k_{vib} \approx (1-6)k_{HS}$,[51] indicating that there may be a large contribution from k_{ph}.

While Eqs. and are commonly used to establish a high-scatter limit for diffusivity and thermal conductivity, predictions for a-SiGe alloys demonstrated that these are not true high-scatter limits.[14] Recently, the thermal conductivity of several materials has been measured to be significantly below k_{HS}.(cite)

By using lattice dynamics calculations and molecular dynamics simulations, we predict the inputs to Eq. (1) in Sections IV A, IV B, and IV D. The thermal conductivity k_{vib} is predicted in Section V. The MFPs of phonons and diffusons are predicted the thermal conductivity accumulation is predicted in Section V B.

ENDALAN

III. CALCULATION DETAILS

BEGINALAN

A. Sample Preparation

We discuss the sample preparations...There are several methods available which can use empirical and ab-initio-derived interatomic potentials. (cite) We use models for a-SiO2 and a-Si which have been used previously in the literature.(cite)

1. *Amorphous Si*

For a-Si, we use models created by the Wooten-Winer-Weaire (WWW) algorithm in Ref. 52. Sample sizes with N_a = 216, 1000, 4096, and 100,000 were provided, where N_a are the number of atoms in the disordered supercell.(cite) A large sample was created from the $N_a = 100,000$ sample by treating it as a unit cell and tiling twice in all directions to create an $N_a = 800,000$ sample with box size L nm. All a-Si structures used have a density ρ equivalent to the perfect crystal with a lattice constant of a =5.43 $\mathring{A}$.(cite)

The Stillinger-Weber potential is used with these samples. The samples were annealed at a temperature of 1100 K for 5 ns to remove meta-stability. Amorphous materials have many different atomic (potential energy) configurations with nearly equivalent energies.[53,54] The removal of meta-stability is demonstrated by an increase in the predicted sound speeds, $v_{s,T}$ and $v_{S,L}$, after annealing (see Table).[54] This meta-stability can cause errors when predicting vibrational lifetimes using Normal Mode Decomposition (NMD, see Section IV C).(cite)

Similar lifetimes can be obtained with a-Si samples created using a melt-quench-anneal procedure(cite), see Section III A.

(footnote)In an amorphous material, there are many potential energy configurations (atomic positions) which are nearly equivalent in energy. At a sufficient temperature, the meta-stable configurations cause the equilibrium atomic positions to vary in time. This can effect on the prediction of the vibrational mode lifetimes when using the normal mode decomposition method. In the time domain, the average normal mode potential and kinetic energy must be calculated and subtracted from the normal mode energy autocorrelation function.(cite) If the average energy is not specified correctly, unphysically large or small mode lifetimes can be predicted.(cite)

(footnote) The entire procedure is performed at constant volume. Crystalline silicon (c-Si) is first melted at a temperature of 10,000 K. The liquid is then quenched instantaneously to 300 K, and then annealed at 1100 K for 10 ns to remove meta-stability.

2. *Amorphous SiO_2*

The a-SiO_2 samples are used from Ref. 39 and have size N_a = 288 , 576, and 972. The atomic potentials used for a-SiO_2 are the same as in Ref. 39 except the 24-6 Lennard-Jones

potential is changed to a 12-6, which has a negligible effect on the predictions presented in this paper. Larger systems of N_a = 2880, 4608, and 34562 are created by a similar melt-quench technique as that used in Ref. 39

(footnote) The entire procedure is performed at constant volume. Crystalline silicon (c-Si) is first melted at a temperature of 10,000 K. The liquid is then quenched instantaneously to 300 K, and then annealed at 1100 K for 10 ns to remove meta-stability.

B. Simulation Details

Molecular dynamics simulations are performed using the disordered a-SiO_2 and a-Si supercells described in Section III A. The MD simulations were performed using LAMMPS[55] with time steps of dt = 0.00905 , 0.0005 for a-SiO_2 and a-Si. Ten MD simulations with different initial conditions were run for 2^21 time steps and the atomic trajectories sampled ever 2^8 time steps. For the GK method, the thermal conductivity k_{GK} is predicted by window averaging the integral of the heat current autocorrelation function (HCACF).(cite) For a-SiO_2 and s-Si, a interval of the the HCACF integral can be found which is constant within the statistical noise.(cite) Large system sizes up to N_a = 34,000 and 800,000 can be used to predict k_{GK} for a-SiO_2 and a-Si (see Section III A 1). For smaller systems, the trajectories from the MD simulations used for the GK method are also used in the NMD method to predict the vibrational mode lifetimes (Section IV C).

For the amorphous supercells studied, the only allowed wave vector is the gamma-point (i.e., $\boldsymbol{\kappa} = 0$), where $\boldsymbol{\kappa}$ is the wavevector and there are $3N_a$ polarization branches labeled by ν. Calculation of the vibrational modes at the Gamma point require the eigenvalue solution of a dynamical matrix of size $(3N_a)^2$ that scales as $[(3N_a)^2]^3$, limiting the system sizes that can be considered to N_a = 4608 and 4096 for a-SiO_2 and a-Si. This eigenvalue solution is also required to perform the NMD (see Section IV C) and AF calculations (see Section IV D). The frequencies and eigenvectors were computed using harmonic lattice dynamics calculations and GULP.[56] The calculation of the AF diffuson thermal diffusivities (Eq. (10)) is performed using GULP and a Lorentzian broadening of $5\delta\omega_{avg}$ and $14\delta\omega_{avg}$ for a-Si and a-SiO^2, where $\delta\omega_{avg}$ is the average mode frequency spacing.(cite) Varying the broadening around these values does not change the resulting thermal conductivity k_{AF} significantly (see Section).

ENDALAN

IV. VIBRATIONAL PROPERTIES

A. Density of States

BEGINALAN

In this section, we examine the frequencies and density of states (DOS) for the vibrational modes of a-SiO_2 and a-Si. The vibrational DOS is computed by

$$DOS(\omega) = \sum_i \delta(\omega_i - \omega), \tag{13}$$

where a unit step function is used to broaden $\delta(\omega_i - \omega)$.(cite) The DOS for a-$SiO_2$ and a-Si are plotted in Fig. 1 using two values of broadening, $10\delta\omega_{avg}$ and $100\delta\omega_{avg}$. Because of the finite model size, the low-frequency modes are sparse and the DOS has a large variability dependent on the broadening.[16] As the system size L is increased, the lowest frequency mode will continue to decrease and the gaps in frequency will fill in.(cite) The DOS for a-Si is similar to the DOS of crystalline silicon,[41,57] particularly at low-frequency, and with pronounced features as in disordered lattices.[49,58] The DOS for a-SiO_2 is essentially constant over most of the frequency-range, except at the lowest frequencies.

While the DOS has a large amount of variability at low frequency, there is a clear scaling of $DOS \propto \omega^{-2}$ for both a-Si and a-SiO_2. The range of this scaling is larger for a-Si than a-SiO_2. By fitting the DOS from Fig. 1 to Eq. (9), a sound speed is predicted and reported in Table I and discussed in Section IV A. The Debye model predicts that the contribution from the larger longitudinal sound speed compared to the smaller transverse sound speed will scale as the difference cubed. For a-Si, the contribution from longitudinal modes to the Debye DOS is nearly an order of magnitude less than the transverse modes for a given frequency interval. For a-SiO_2, the longitudinal and transverse sound speeds are closer.(cite experimental DOS)

The intensity of the structure factors are directly proportional to the DOS.(cite) The intensity for the dynamic structure factor of transverse polarizations has been found to be four to five[59] and 6-8[60] times larger than longitudinal polarizations for a models of a-SiO2, which supports our finding that the DOS is dominated by transverse modes.

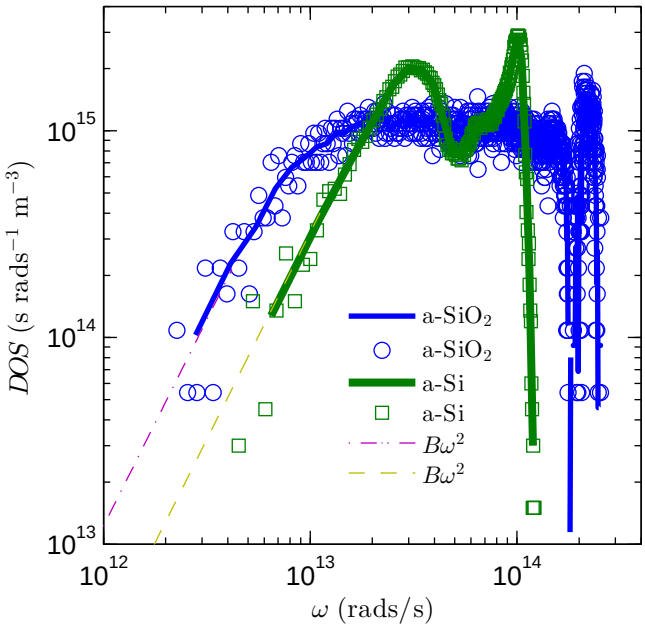

FIG. 1: Vibrational DOS predicted for our models of a-SiO2 and a-Si using Eq. (13). Both models show a scaling at low frequency $DOS(\omega) \propto \omega^{-2}$, which is predicted by the Debye approximation (Eq. (9)) using the transverse sound speeds predicted using various methods (Table I). At high frequency, the DOS of a-SiO2 shows a plateau and then a sharp feature corresponding to a gap in the vibrational spectrum due to the Si and O bonds.(cite) For a-Si, there are two sharp peaks, which show as small peaks in the predictions of the vibrational mode lifetimes (Fig. 3) and mode diffusivities (Fig. 4).

ENDALAN

The observation that the acoustic modes are located on top of a flat background for intermediate values of q has re- cently been found by G otze and Mayr as an essential result in their analytic calculation of the spectra within mode-coupling theory.[61]

The DOS predicted for a-SiO2 is similar to previous models[59] as well as experimentally measured DOS.(cite)

The DOS predicted for jammed systems are similarly dominated by the transverse sound speed,[62] while results for disordered lattices demonstrate[49,58]

B. Group Velocity

BEGINALAN

In the previous section, we examined the low-frequency DOS and found a Debye scaling is a good fit to the data. From

By fitting the DOS from Fig. 1 to Eq. (9), a sound speed is predicted. For both a-Si and a-SiO_2, the sound speeds predicted from the DOS are close to the transverse sound speeds predicted from the elastic constants and the structure factor.

The sound speeds predicted for a-Si in Table are in good agreement with those found in a previous study using a similar model.[14,16]

For a disordered solid, the three acoustic group velocities (two transverse and one longitudinal) can be predicted using the elastic constants[56] or by finite differencing of the three lowest frequency branches of the dispersion relation of the supercell.[14,16,19,40,41,49,63] Except for this low-frequency behavior, there is not an accepted method to predict the group velocity of a vibrational mode in a disordered system, although there have been attempts.[19,40,41,50,64] In the Cahill-Pohl (CP) model, for example, the group velocity of all disordered modes is the sound speed, v_s, which is also assumed for the HS model Eq. (**??**).[50] This assumption is not generally valid for any material.[16,19,40,41,49,64]

The transverse and longitudinal sound speeds of a material can be related to the material's elastic constants, which determine the bulk (G) and shear (K) moduli.(cite) The transverse sound speed is given by(cite)

$$v_{s,T} = \frac{G}{\rho}^{1/2}, \tag{14}$$

and the longitudinal by

$$v_{s,L} = \frac{4G + 3K}{3\rho}^{1/2}. \tag{15}$$

We use the bulk and shear moduli defined in terms of the elastic constants according to the Voight convention.(cite) The sound speeds calculated from the elastic constants are reported in Table . It is clear that the DOS of our models for a-Si and a-SiO_2 are characterized by using the transverse sound speeds, rather than an averaging of the transverse and longitudinal which is commonly used,(cite)

$$v_s = \frac{2}{3}v_{s,L} + \frac{1}{3}v_{s,T}. \tag{16}$$

This is backed up by theoretical(cite) and experimental(cite) results.

The sound speeds can also be estimated from the structure factor.(cite) Calculating the structure factors of the supercell Gamma modes is a method to test for their plane-wave character at a particular wave vector and polarization.[16,65] The structure factor has been used to predict effective dispersion amorphous materials experimentally[66] and numerically.[16,67] The structure factor at a wave vector $\boldsymbol{\kappa}$ is defined as[65]

$$S^{L,T}(\tbinom{\boldsymbol{\kappa}}{\omega}) = \sum_{\nu} E^{L,T}(\tbinom{\boldsymbol{\kappa}}{\nu})\, \delta(\omega - \omega(\tbinom{\boldsymbol{\kappa}=\mathbf{0}}{\nu})), \tag{17}$$

where the summation is over the Gamma modes, E^T refers to the transverse polarization and is defined as

$$E^{L}(\tbinom{\boldsymbol{\kappa}}{\nu}) = \left| \sum_{b} \hat{\boldsymbol{\kappa}} \cdot e(\tbinom{\boldsymbol{\kappa}=\mathbf{0}\ b}{\nu\ \alpha}) \exp[i\boldsymbol{\kappa} \cdot \boldsymbol{r}_0(\tbinom{l=0}{b})] \right|^2 \tag{18}$$

and E^L refers to the longitudinal polarization and is defined as

$$E^{T}(\tbinom{\boldsymbol{\kappa}}{\nu}) = \left| \sum_{b} \hat{\boldsymbol{\kappa}} \times e(\tbinom{\boldsymbol{\kappa}=\mathbf{0}\ b}{\nu\ \alpha}) \exp[i\boldsymbol{\kappa} \cdot \boldsymbol{r}_0(\tbinom{l=0}{b})] \right|^2 . \tag{19}$$

In Eqs. (18) and (19), the b summations are over the atoms in the disordered supercell, $\boldsymbol{r}_0(\tbinom{l=0}{b})$ refers to the equilibrium atomic position of atom b in the supercell, l labels the unit cells ($l = 0$ for the supercell), α labels the Cartesian coordinates, and $\hat{\boldsymbol{\kappa}}$ is a unit vector. Explicit disorder is included in the Gamma frequencies $\omega(\tbinom{\boldsymbol{\kappa}=\mathbf{0}}{\nu})$ and the $3N_a$ components of the eigenvectors, $e(\tbinom{\boldsymbol{\kappa}=\mathbf{0}\ b}{\nu\ \alpha})$.

The structure factors $S^{L,T}(\kappa, \omega)$ are plotted in Fig. 2 for a-SiO_2 and a-Si (left and right panels) for wavevectors along the [100] direction of the supercells. The length scale used for the wavevectors, $\kappa = 2\pi/a[100]$, are $a = 4.8$ and 5.43 $\mathring{A}$ for a-SiO_2 and a-Si, which are based on the lattice constants of c-SiO2 and c-Si.(cite) Frequencies $\omega_0(\kappa)$ and lifetimes $\Gamma(\kappa)$ are predicted by fitting each structure factor peak $S^{L,T}(\tbinom{\boldsymbol{\kappa}}{\omega})$ to a Lorentzian function

$$S^{L,T}(\tbinom{\boldsymbol{\kappa}}{\omega}) = \frac{C_0(\boldsymbol{\kappa})}{[\omega_0(\boldsymbol{\kappa}) - \omega]^2 + \Gamma^2(\boldsymbol{\kappa})}, \tag{20}$$

where $C_0(\nu)$ is a constant related to the DOS.[58] A dispersion relation is identified by plotting $\omega_0(\kappa)$ in the middle panel of Fig.2, where the error bars indicate the peak widths $\Gamma(\kappa)$.

For a-Si, the peaks are reasonably Lorentzian for all wavenumbers considered.[68] For a-SiO2, the peaks are well-approximated as Lorentzian only at the smallest wavenumbers. For large wavenumber, the structure factors peaks are much less than an order of magnitude

larger than the background, and the widths are on the order of the frequency range considered in Fig. 2.(cite) The structure factor gives the frequency spectrum needed to construct a (nonstationary) propagating state with a pure wave vector Q and pure longitudinal or transverse polarization[14]. Only low-frequency vibrations have an (approximate) wavevector in disordered systems, and there is no theorem guaranteeing this.[16] While the structure factor gives the frequency spectrum needed to construct a propagating state with pure wavevector $\boldsymbol{\kappa}$, the mode spectrum $E^{T,L}(\overset{\boldsymbol{\kappa}}{\nu})$ (Eqs. and) predicts the plane-wave character of each mode.(cite) As shown previously, it is not possible in general to assign a unique wavevector to individual modes, even at low frequency,[14,69,70] which makes predicting individual mode group velocities challenging. Attempts have been made to predict individual mode group velocities, but it is not clear that these methods are consistent with the predictions made by the structure factor, in this work and in others.(cite)

Fig 4 shows the dispersion extracted by locating the peaks in the structure factor for a-SiO2 and a-Si. For a-Si, the dispersion is nearly linear at small κ with slight negative dispersion at high κ.(cite) For a-SiO2, the dispersion is negative for even the smallest wavenumbers considered, transitioning to a strong positive dispersion at intermediate wavenumber. For intermediate κ the longitudinal dispersion for a-SiO_2 more closely resembles the so-called "dispersion law for diffusons", where $\omega \propto q^2$.[58] This large positive dispersion has been observed in various amorphous models[68] including of a-SiO2.[71]

Sound speeds are estimated from the structure factor peaks by finite differencing,

$$v_s = \frac{\delta\omega_0(\kappa)}{\delta\kappa}. \tag{21}$$

Estimates of the sound speeds are found from using finite difference of the peaks in $S_{T,L}$ are shown in Table using the lowest frequency peaks from Fig. 2. The values obtained from the elastic constants are somewhat larger, an indication of the negative dispersion seen at low *wavenumber*, particularly for a-SiO2. It is clear that negative dispersion also affects the low-frequency DOS, where the predicted sound speed $v_{s,DOS}$ is less than that predicted from the structure factor, which is less than that predicted from the elastic constants (Table). The transverse sound speed predicted by the DOS $v_{s,DOS}$ is used for both a-SiO_2 and a-Si throughout the rest of this work.

ENDALAN

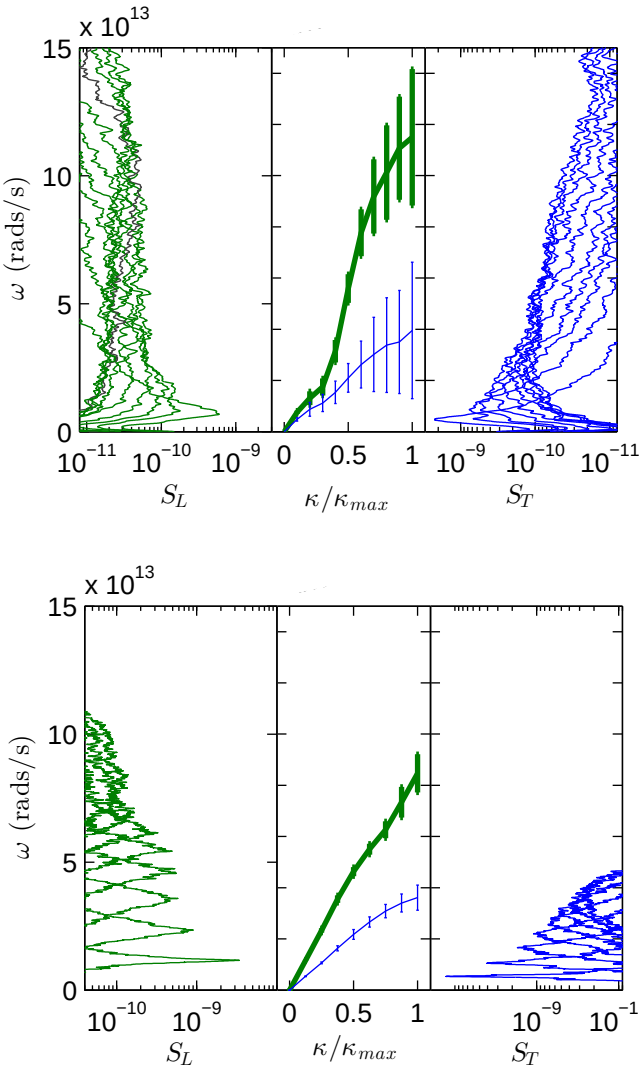

FIG. 2: Longitudinal (left panel) and transverse (right panel) structure factors (Eq. (17)) for a-SiO2 (top plot) and a-Si (bottom plot). Sound speeds are estimated by finite differencing (Eq. (21)) of the lowest frequency peaks and are reported in Table I. The dispersion for a-SiO2 is only linear for the lowest frequency, smallest wavenumbers. The dispersion for a-Si is linear over a wider range of wavenumber. Lifetimes are predicted from the widths of the structure factor peaks (Eq. (20)) and are plotted in Fig. 3.

C. Mode Lifetimes

BEGINALAN

We now predict the lifetimes of all vibrational modes in our models of a-SiO2 and a-Si

TABLE I: Estimated from the elastic constants, the pre-annealed group velocities are $v_{s,T,} = 3,670$, $v_{s,L,elas} = 7,840$ for a-Si and $v_{s,T,elas} = 2,541$, $v_{s,L,elas} = 4,761$ for a-SiO2 (see Section IV B).

method	Eqs. (14), (15)	Eqs. (17), (21)	DOS Eq. (9)
a-SiO_2			
transverse	3,161	2,732	2,339
longitudinal	5,100	4,779	
a-Si			
transverse	3,886	3,699	3,615
longitudinal	8,271	8,047	

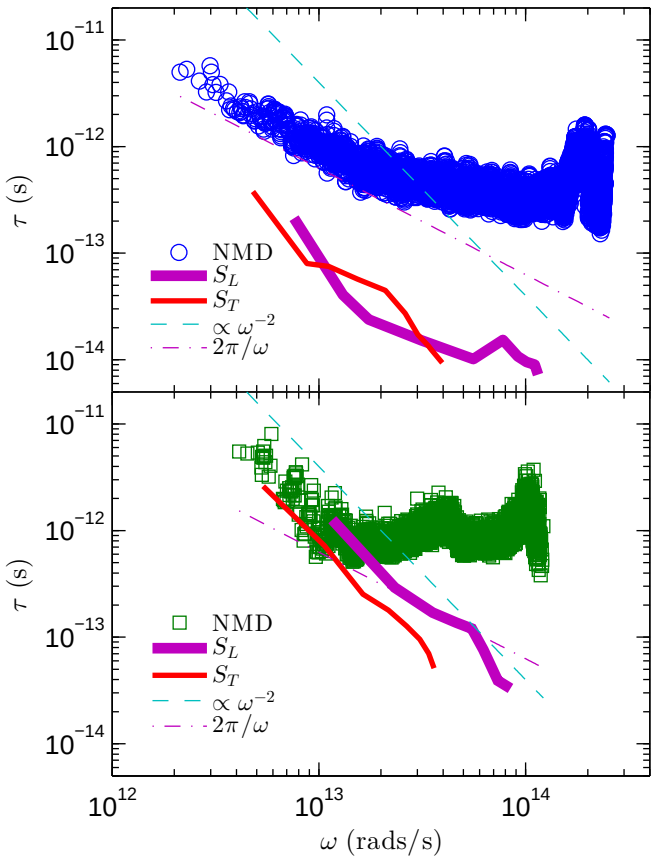

FIG. 3: vibrational mode lifetimes predicted by NMD (Eq. (25)) and the structure factors (Eq. (20)) for a-SiO2 (top plot) and a-Si (bottom plot). The IR limit is a lower limit for the mode lifetimes, while the lifetimes from the structure factors fall below this limit, particularly for a-SiO2. The structure factor lifetimes generally follow a scaling $\tau \propto \omega^{-2}$ for both systems, while the mode lifetimes show a plateau before crossing the IR limit.

to compare with lifetimes predicted from the structure factor (Eq. (20)). We use the MD simulation-based normal mode decomposition (NMD) method to predict the lifetimes of each vibrational mode in the disordered supercell for our models of a-SiO2 and a-Si.[72–75] The NMD method can predict vibrational lifetimes which are affected by the disorder in the supercell.(cite)

In NMD, the atomic trajectories from MD simulations are first mapped onto the vibrational mode coordinate time derivative,[37]

$$\dot{q}(\substack{\boldsymbol{\kappa}=\mathbf{0}\\ \nu};t) = \sum_{\alpha,b,l}^{3,n,N} \sqrt{\frac{m_b}{N}} \dot{u}_\alpha(\substack{l\\ b};t)\, e^*(\substack{\boldsymbol{\kappa}=\mathbf{0}\ b\\ \nu\ \ \alpha}) \exp[i(\mathbf{0}\cdot\mathbf{r}_0(\substack{l\\ 0}))]. \tag{22}$$

Here, m_b is the mass of the b_{th} atom in the unit cell, u_α is the α-component of the atomic displacement from equilibrium, $\dot{u}_\alpha$ is the α-component of the atomic velocity, and t is time. The spectral energy of each vibrational mode, $\Phi(\substack{\boldsymbol{\kappa}\\ \nu};t)$, is calculated from

$$\Phi(\nu,\omega) = \lim_{\tau_0\to\infty} \frac{1}{2\tau_0} \left| \frac{1}{\sqrt{2\pi}} \int_0^{\tau_0} \dot{q}(\substack{\boldsymbol{\kappa}=\mathbf{0}\\ \nu};t) \exp(-i\omega t) dt \right|^2. \tag{23}$$

The vibrational mode frequency and lifetime is predicted by fitting each mode's spectral energy $\Phi(\nu,\omega)$ (see Appendix) to a Lorentzian function

$$\Phi(\nu,\omega) = \frac{C_0(\nu)}{[\omega_0(\nu)-\omega]^2 + \Gamma^2(\nu)}, \tag{24}$$

where the constant $C_0(\nu)$ is related to the average energy of each mode and the linewidth $\Gamma(\nu)$.[75] The mode lifetime is given by(cite)

$$\tau(\nu) = \frac{1}{2\Gamma(\nu)} \tag{25}$$

The NMD-predicted lifetimes are plotted in Fig. 3 for a-SiO2 and a-Si. For both a-SiO2, the mode lifetimes are generally larger than the IR limit $\tau = 2\pi/\omega$,(cite) and follow this limit at low frequency. There is no clear evidence for a quadratic scaling $\tau \propto \omega^{-2}$, which corresponds to a quadratic scaling of the diffusivity at low frequency where the group velocity is constant (Eq. (4)). At high frequency the mode lifetimes are roughly constant without definite scaling. There is a peak near 2 10^{14} rads/s which corresponds to a peak in the DOS (see Fig. 1). The lifetimes predicted from the structure factor fall below the NMD-predicted lifetimes and the IR limit. This is because the structure factor for a-SiO2 is evaluated for large enough wavenumber that the peaks are not well-approximated as Lorentzian.(cite)

Fitting the peaks we find the linewidth (inverse lifetime) to be on the order of the frequency range considered in Fig. 2. Models(cite) and theoretical(cite) predictions show that the structure factor begins to take on the form of the DOS for large enough wavenumber.[24,76]

For a-SiO2 the NMD and structure factor-predicted lifetimes indicate that the low-frequency modes in our model are not well-characterized as propagating.(cite) For a-Si, The mode lifetimes show a clear scaling at low frequency $\tau \propto \omega^{-2}$. The lifetimes plateau at higher frequencies, over a wider range of frequencies than a-SiO2, with two peaks corresponding to peaks in the DOS (Fig. 1). The plateau of lifetimes at high frequencies has been reported for disordered lattices[49,77] and other models of a-Si.[40] The transition from the quadratic low-frequency scaling to the plateau region occurs near 1 10^{14} rads/s, which corresponds to where the DOS peaks in Fig. 1. Similar behavior was observed for models of disordered lattices.[49] The lifetimes predicted by the structure factor are in good agreement with those predicted by NMD at low frequencies. Similar agreement has been reported in other models of topologically disordered materials.[78] The longitudinal and transverse polarizations outline the scatter in the NMD-predicted lifetimes. While the DOS is dominated by transverse modes, the NMD and structure factor-predicted lifetimes indicate there is some mixture of longitudinal and transverse-like modes at low frequencies.(cite) Using the transverse sound speeds predicted from the DOS $v_{s,DOS}$ (Table), the NMD-predicted lifetimes are used to predict the mode diffusivities in the next section.

The NMD-predicted lifetimes in this work are similar in magnitude to those predicted for previous models of a-Si. Fabian finds lifetimes on the order of picoseconds for a-Si and para-crystalline silicon.[79,80] A previous study of Tersoff a-Si predicted vibrational lifetimes on the order of 100 ps, about ten times the values reported here and in other studies.(cite) It is unclear what the source of this discrepancy is. Using the Tersoff potential on the WWW models in this work we find...Predicted lifetimes are also similar for samples created using a melt-quench technique (see Section III A 1).

ENDALAN

A numerical investigation of Bickham[81] indeed shows that a strong perturbation of the vibrational spectrum of a-Si can relax on a 100 ps time scale, compared to 10 ps for a weak perturbation.[82]

The lifetimes found by this method are in good agreement with the perturbative calculations of Fabian and Allen and are on the order of 10 ps at low tem- peratures in both 216

and 4096 atom supercells.[82]

Our results indicate that all of these processes occur on a much faster time scale than the 1 ns temporal resultion of the Raman experiments, so it is not obvious that the measured relaxation rates should be identified with vibrational lifetimes.[81]

D. Diffusivities

BEGINALAN

Based on the lifetimes predicted from NMD, the diffusivities D_{NMD} predicted at low frequency for a-Si follow very closely the scaling $D(\omega) \propto \omega^{-2}$ (Fig. 4). Rayleigh scattering due to point defects predicts $D \propto \omega^{-4}$, but is not observed in the amorphous systems studied in this work.(cite) While quartic scaling has been observed in harmonic studies of the diffusivities of modes in disordered lattices and jammed systems,[62,77,85] it has been demonstrated that the harmonic disorder in a-Si produces a scaling similar to Umklapp scattering.[14]

The mode diffusivities show much less scatter than those predicted by the AF theory D_{AF}, which is due to the finite-size system and the broadening which is required to evaluate Eq. (10).[14] By using a much larger broadening ($100\delta\omega_{avg}$) the scatter in the AF-predicted diffusivities at low frequency can be smoothed, but at the cost of decreasing the diffusivities at intermediate and high frequencies. It is possible that a frequency-dependent broadening may be necessary for a-Si, but determining this dependence is not clear nor necessary for interpreting the results in this work.

Both a-SiO_2 and a-Si have a region at higher frequencies where the AF-predicted mode diffusivities are relatively constant. This behavior has been reported for a number of model disordered systems such as disordered lattices[49,58,77], amorphous solids,(cite) and jammed systems.(cite) At the highest frequencies the AF-predicted diffusivities trend exponentially to zero, which is an indication that these modes are "locons", spatially localized modes which do not contribute to thermal conductivity.[65,84]

For a-SiO2, we find the same $\omega_{cut} = 4.55$ rad/s as used in Ref 24 and a quadratic scaling gives a reasonably good fit to the low-frequency diffusivities predicted by the AF theory (Fig. 4). In this work, the predicted contribution $k_{ph} = 0.10$ W/m-K is close to that predicted by Ref. 24. Within the errors of the predictions, the predicted k_{ph} for a-SiO2 is not significant,

contributing about 5% to k_{vib}.

Because the AF-predicted diffusivities show a large scatter for a-Si at low-frequencies, both ω^{-2} and $\omega-4$ scalings can be considered as "fits" to the low-frequency behavior. Both FKAW experimental results by Cahill et al. have used ω^{-4} scaling at low frequency.

Using the NMD-predicted lifetimes and AF-predicted diffusivities, a representative velocity can be computed,

$$v_{AF}(\omega) = \left(3\frac{D_{AF,i}(\omega)}{\tau(\omega)}\right)^{1/2}, \tag{26}$$

and is shown in the inset of Fig. 5. For a-Si, v_{AF} follows a decreasing trend with increasing frequency, similar to the trend for group velocities in a simple monatomic crystal.(cite)

The dependence of v_{AF} in frequency is similar to that found for simple crystalline systems, where negative dispersion typically causes a decrease of group velocity with increasing frequency (or wavevector).(cite) Negative dispersion has been predicted by many models of both a-SiO2 and a-Si,[86] as have experimental measurement of dispersion relations.(cite) The effective group velocities which have been predicted using dispersion relations near zero wavevector for large supercells of amorphous[19,40] and disordered lattices[63] would appear to be underestimates compared with the effective velocities v_{AF} predicted in this work, where v_{AF} is within a factor of three of v_s for all but the highest frequency, localized modes.(cite) Our predictions for v_{AF} also support the notion of a minimum thermal diffusivity on the order of D_{HS} for all vibrational modes except those which are localized (the so-called "locons").(cite)

ENDALAN

This choice of ω_{cut} is motivated by the AF predictions, gives a reasonable fit to the NMD predictions, and also an extrapolated total thermal conductivity k_{vib} which is in reasonably good agreement with k_{GK} (Fig. 6).

Based on the NMD-predicted diffusivities, the modes at low frequency are dominated by transverse modes. However, given the scatter in the NMD-predicted lifetimes, there is some mixture of transverse and longitudinal modes at low frequency. Treating these two branches separately is not necessary since similar results are obtained by assuming a single branch scaling $D(\omega) = B\omega^{-2}$ which is fit to coincide with the peak in diffusivity D_{AF} at $\omega_{cut} = 11.6$ E 12 rads/s. This choice of ω_{cut} is close to that used by FAB ($\omega_{cut} = 9.65$ E 12 rads/s),[14] and is somewhat smaller than that used by FKAW[16] and Cahill et al.[15] ($\omega_{cut} = 15.2$ E 12

rads/s).

The lifetimes predicted by NMD and scaled by the sound speed diverge from the AF predicted mode diffusivities when the mode lifetimes approach the IR limit, shown in Fig. 3. This is an indication that the modes have transitioned from propagating (where the diffusivity D and lifetime are related by $D = (1/3)v_s^2\tau$) to non-propagating where D and τ need not be related.[14,16,43,48]

which generally agree with diffusivities computed according to the formula of Edwards and Thoules.[16,58,83]

Thermal diffusivity has been predicted using a wave-packet method

It was shown

Garber shows that these high-frequency modes are localized in the Anderson sense, showing exponential decay of the mode eigenvector.[84]

It was shown that the diffusivity $D_{AF}(\omega) \propto DOS(\omega)$ at low frequency when the modes are spatially uncorrelated and the overlap between them is small and independent of the frequency.[62,85] This result helps to explain the plateau of diffusivity for both a-SiO2 and a-Si at higher frequencies. The features in $D_{AF,i}$ for both a-SiO2 and a-Si can be explained by peaks in the DOS at these frequencies.

E. Mean Free Paths

Using the lifetimes predicted from the structure factor peaks and the transverse sound speed, the MFP is about the size of the simulation cell L.

$$\Lambda_{AF}(\omega) = (3D_{AF,i}(\omega)\tau(\omega))^{1/2}, \tag{27}$$

V. THERMAL CONDUCTIVITY

A. Bulk

BEGINALAN

To predict the bulk thermal conductivity for our models of a-SiO2 and a-Si, we use Eq. (1) and the GK method.(cite) The GK method for predicting thermal conductivity is

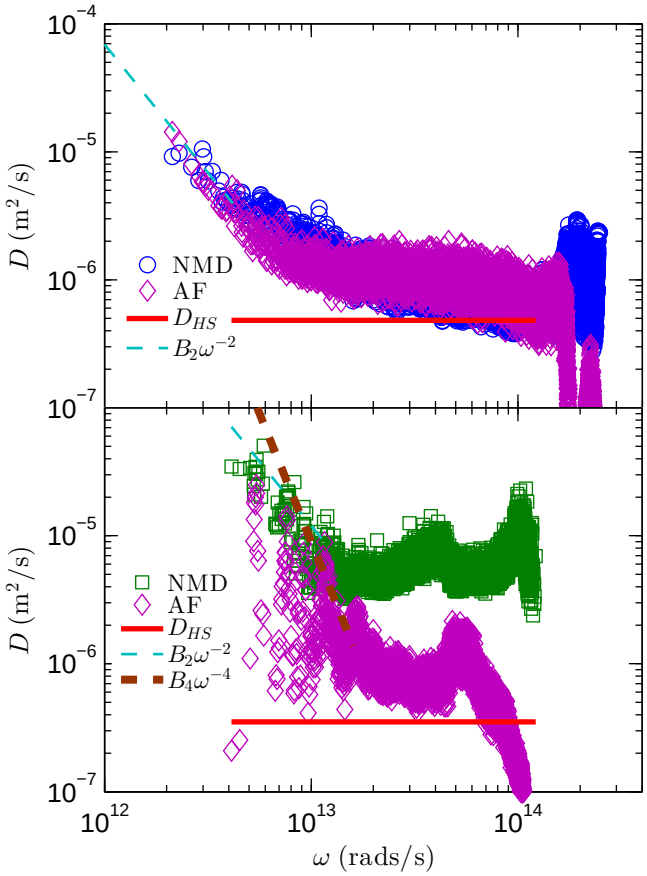

FIG. 4: vibrational mode diffusivities predicted from NMD (using Eqs. (4) and (25) with the sound speed $v_{s,DOS}$ from Table I) and AF theory (Eq. (10)). Also shown are the extrapolations Eqs. (7) and (8), which are used with Eq. (2) to predict the thermal conductivity accumulations in Fig. 8, and the high-scatter limit Eq. (11).

relatively inexpensive compared to the NMD and AF methods so large system sizes can be studied (see Section III A 1). Similarly large systems were studied in Ref. 40. The details of the GK method are discussed in Section III B.

The GK-predicted thermal conductivity k_{GK} is plotted in Fig. 6 for varying system sizes L. For a-SiO2, there is no apparent dependence of k_{GK} on L. For a-Si, there is a clear dependence of k_{GK} on L. Assuming the DOS has the form of Eq. (9) and the diffusivity scaling is quadratic (Eq. (7)) for the low-frequency modes in the system, the thermal conductivity as a function of the system size takes the form

$$\frac{k(L)}{k_{bulk}} = 1 - \frac{c_0}{L}, \tag{28}$$

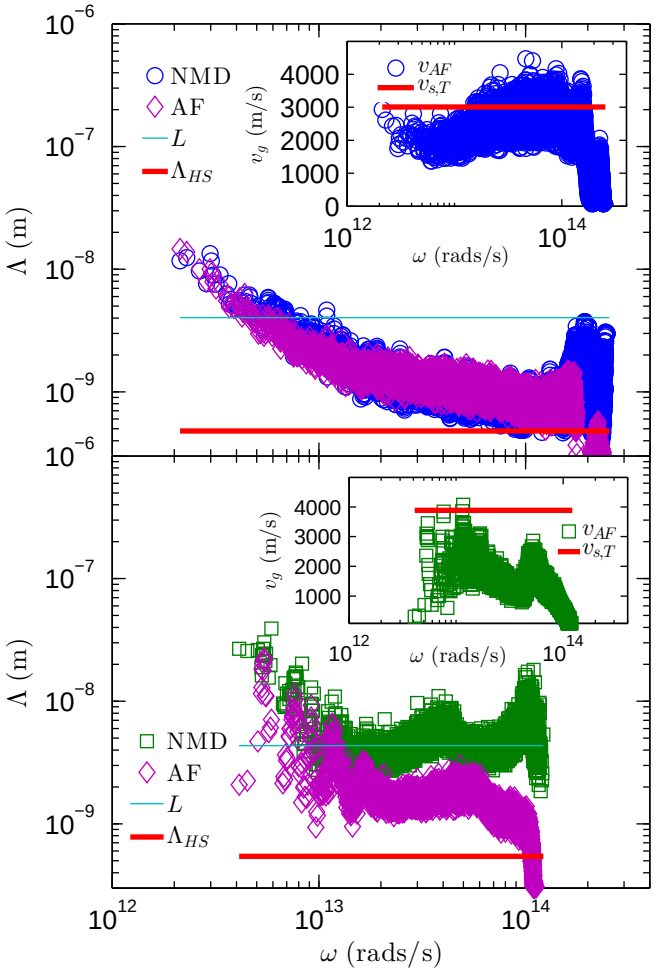

FIG. 5: vibrational MFPs predicted from NMD using Eq. (6) and the sound speed predicted in Table I and from NMD and AF using Eq. (27). Good agreement between the two methods is seen at low frequency, indicating that the modes are propagating and Eqs. (4) and (5) are valid. The majority of MFPs in the intermediate the high-frequency range lie between the simulation box size L and the bond distance a. The inset compares the representative mode velocities Eq. (26) and the sound speeds. For a-Si, v_{AF} decreases with increasing frequency, similar to the behavior of a monatomic crystal.(cite) The MFPs and mode velocities only approach zero at the highest frequencies, which is an indication that the modes are localized.

where k_{bulk} is the extrapolated bulk thermal conductivity and c_0 is a constant. The extrapolation is performed using the three largest system sizes studied, including the tiled 800,000 atom sample (see Section III A 1). We do not observe that tiling an a-Si model increases the

thermal conductivity of a given system size above that predicted by Eq. , as was found in Ref 19. This is likely due to the small (512 atom) model used to perform the tiling in that study, while we use a 100,000 atom model. The success of Eq. (28) for the dependence of k_{GK} on L for our model is in agreement with the quadratic scaling of the diffusivity for a-Si shown in Fig. 4 and the Debye-scaling of the DOS in Fig. 1.

To predict k_{vib} we choose ω_{cut}, the constant B for the diffusivity scaling, and the sound speed v_s. For both a-SiO2 and a-Si, we use the sound speeds predicted by a fit to the low-frequency DOS (Fig. 1). For a-Si, the constant B for the quadratic scaling is chosen such that $D(\omega) = D_{AF,i}$ for $\omega_i = 1.16$ rad/s. This value of ω_{cut} is somewhat smaller than that used in Ref and . The constant B we find is somewhat larger than that found in Ref. and . We choose this ω because of the reasonable agreement between the AF-predicted D_{AF} and NMD-predicted D_{NMD} in this frequency region, shown in Fig. 4. We predict for a-Si $k_{ph} = 0.62$ W/m-K. Similar values for k_{ph} can be predicted by increasing ω_{cut} and decreasing B.

For a-Si a quadratic scaling is also considered using ω_{cut} from the study by . As there is no clear evidence of a quartic scaling of diffusivity, we choose the constant B to pass visibly through both D_{AF} and D_{NMD} in Fig. 4 because there is no clear procedure to perform a fit. Our choice of $B = 9.010^{46}$ m$^{@}$/s (rads/s)$^4 for the quartic scaling is nearly the same as a fit^{?} to the diffusivities in Ref$ 14,B=1.23 10^{47} m$^{@}$/s (rads/s)^4.$When using the quartic diffusivity scaling$D($\omega$) $\propto$ ω^{-4}, the thermal conductivity is divergent as the frequency goes to zero. (cite) The thermal conductivity can be made finite using a boundary scattering models,(cite) such as the simple one considered in Section V A. While a fit to our model is not possible for the quartic scaling, it has been used to explain previous experimental measurements of a-Si thin films.(cite)

Baldi et al used a $\omega_{cut} = 4.55$ rads/s, which is a reasonable cut-off for our model of a-Si.[24] Baldi et al find that the contribution k_{ph} 0.1 W/m-K, which is the same as the contribution k_{ph} predicted in this work for a-SiO2. This contribution k_{ph} is smaller than the error bars in the predictions of k_{vib} and k_{GK} shown in Figs. and .

The quadratic scaling of mode diffusivities at low frequencies for a-Si is responsible for the system size dependent thermal conductivity predicted by the GK method k_{GK}. While our model is best described by quadratic scaling, we are modeling bulk a-Si.

ENDALAN

Comparing with previous MD simulations of a-Si, Lee found a value of around 1 W/m-K but with very small supercell sizes.[87] He et al find for bulk a-Si $k_{vib} = 3$ W/m-K using the Tersoff potential and a linear extrapolation of the form Eq. using non-equillibrium molecular dynamics.

For smaller system sizes, the same trajectories are used for the GK and NMD methods. The MD simulations were run with the same parameters as the NMD method (see Section).

The predicted thermal condcutivties from the GK method are plotted in Fig. . For a-SiO2, the thermal conductivity is size independent within the errors. For a-Si, there is a clear size-dependance of the thermal conductivity

To compare the results of the mode-based methods (NMD and AF) and the GK method, it is necessary to estimate the missing contribution from vibrational modes with frequency less than the minimum frequency of the finnite systems.

"We find that we cannot define a wave vector for the majority of the states, but the intrinsic harmonic diffusivity is still well-defined and has a numerical value similar to what one gets by using the Boltzmann result, replacing v by a sound velocity and replacing l by an interatomic distance a. "[14]

"In order to fit the experimental sc(T) it is necessary to add a Debye- like continuation from 10 meV down to 0 meV. The harmonic diffusivity becomes a Rayleigh m law and gives a divergent (T) as T O. To eliminate this we make the standard assumption of resonant- plus-relaxational absorption from two-level systems (this is an anharmonic effect which would lie outside our model even if it did contain two-level systems implicitly). "[14]

The same ω_{cut} was used by Cahill et al. together with a Rayleigh scaling and a boundary scattering model to find $k_{ph} = 0.31$ W/m-K.[15]

The relative contribution of k_{ph} and k_{AF} is also predicted to be similar for silicon nanowires.[41]

The comparison between theory and experi- ment supports the description of heat transport in disordered materials developed in Ref. 10, namely, that the dominant heat transport mech- anism is coupling between nearly degenerate, extended, but nonpropagating vibrational modes.

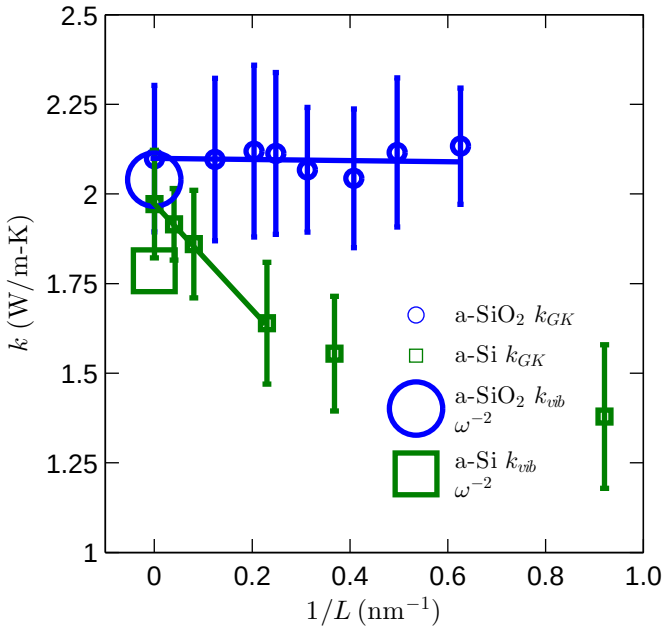

FIG. 6: Thermal conductivities of a-SiO$^2 and a - Si predicted using the GK method. For a - SiO2, the thermal conductivity is size - independent, indicating there is no important contribution from phonons (Eq. Si, there is a clear size dependance, which is accounted for by using Eq. (2) and an ω^{-2} extrapolation (Eq. (7), Fig. 4).

B. Accumulation Function

BEGINALAN

The thermal conductivity accumulation function,

$$k(\Lambda_{cut}) = \frac{1}{V}\int_0^{\Lambda_{cut}} kbD(\Lambda)DOS(\Lambda) + \frac{1}{V}\sum_{\Lambda<\Lambda_{cut}} kbv_{AF}\Lambda_{AF}, \tag{29}$$

is predicted using our models of bulk a-SiO2 and a-Si and shown in Fig. . For the phonon contribution k_{ph}, the mode diffusivities ($D(\omega)$ can be transformed $D(\Lambda) = D(\omega)/v_s$. A simple boundary scattering based on the film thickness t_f and the Matthiesen rule is used,

The thermal conductivity accumulation functions for a-SiO2 and a-Si thin films are shown in Fig. . The thermal conductivity accumulation function for a-SiO2 saturates at a MFP of 10 nm, which is on the order of the finite size of our model (Section III A). This sharp accumulation at small MFPs is in good agreement with the prediction that k_{AF} is the dominant contribution to k_{vib}. This result is also in accord with the penetration depth-independent

thermal conductivity measurements using broadband FDTR.[20] Only the quadratic scaling is considered for a-SiO2, which is discussed later in Section V B.

For a-Si, the thermal conductivity accumulation function shows that k_{AF} saturates before 10 nm, which is also on the order of our finite model size. The propagating contribution k_{ph} is predicted using both quadratic and quartic scaling for the mode diffusivities. As discussed in Section V, the quadratic scaling is responsible for the system size dependent thermal conductivity predicted by the GK method (k_{GK}, see Section V) and seems to be the correct scaling to describe the low-frequency modes for our model of bulk a-Si. Using the quadratic scaling, the thermal accumulation functions for our model of a-Si thin films passes reasonably well through many of the experimentally measured values.(cite) The quartic scaling also passes through many of the experimentally measured values reasonably well, particularly for film thicknesses larger than 10 μm.(cite)

ENDALAN

C. Discussion

BEGINALAN

Previous experimental studies of a-SiO2 have estimated negligible the contribution from low frequency ($\omega < \pi 10^1 2 rads/s$)[88] vibrational modes to be negligible. Using our model of a-SiO2, we also find the low-frequency propagating contribution to be negligible (Section V B). While experiments show there is are cross-over regions from quadratic to quartic scaling of the mode lifetimes in a-SiO2, the thermal conductivity of thin film a-SiO2 shows no significant dependence on the thickness.(cite) The cross-over region from quadratic to quartic, then back to quadratic observed in experiments for a-SiO2 occurs in the frequency range 4.610^9 to 1.5210^{10} rads/s,[23] and $3.0410^1 1$ to 1.5210^{12} rads/s[27]. While these frequency ranges are inaccessible by our finite- size models, we estimate that the extrapolated k_{ph} using a quartic scaling in this region to be...

The transverse sound speed predicted for our model of a-SiO2 is about 85% of that measured by experiment.[17] While using a smaller transverse sound speed leads to an underprediction of the mode diffusivity scalings (Eq. (4), Fig. 4), it leads to an overprediction of the DOS (Eq. (9)). Overall this leads to an underprediction of the thermal conductivity because the DOS scales as $DOS(\omega) \propto 1/v_s^3$. We can regard the predictions from our models,

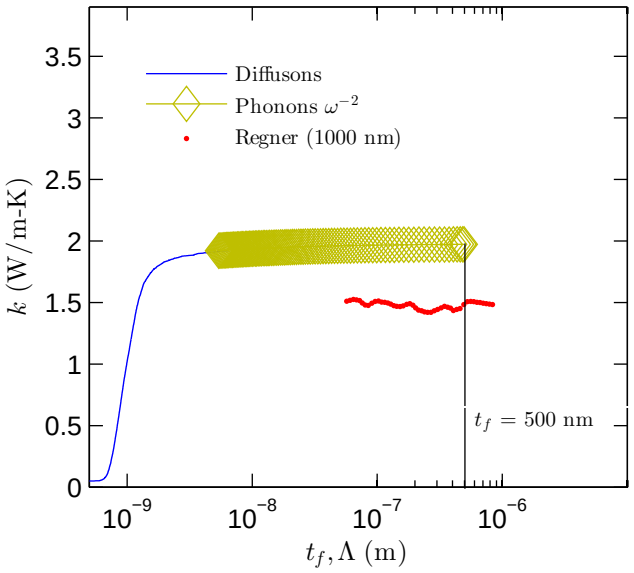

FIG. 7: Thermal conductivity accumulations and thermal conductivities versus film thickness for a-SiO2 (top plot) and a-Si (bottom plot) from: (i) predictions from this work, (ii) recent broadband measurements of Regner et al, (iii) various experimental measurements for a wide-range of a-Si film thicknesses. While the thermal conductivity predictions for a-SiO2 and a-Si in this work seem to be well-characterized by Umklapp type scaling of the MFPs (Eq. (7)), this scaling is not able to predict the dramatic increase of thermal conductivity with increasing film thickness from experimental measurements of a-Si thin films.

with smaller transverse sound speeds, as an upper bound on k_{ph} for a given diffusivity scaling $D(\omega) = B\omega^{-2}$. The critical parameter is the choice of ω_{cut}.(cite) We pick ω_{cut} and the low frequency scaling $D(\omega) = B\omega^{-2}$ based on their ability to describe the low-frequency behavior of the vibrational modes in our finite-size models. The quadratic scaling $D(\omega) = B\omega^{-2}$ has been observed in separate numerical studies for models of a-SiO2(cite) and a-Si(cite).

The bulk thermal conductivity predicted for our model of a-SiO2 overestimates that of experimental measurements.[20] This can be attributed to either difference between experimental a-SiO2 and the potential model used in this work,(cite) the lack of anharmonic scattering included in the AF theory,[14] or the assumption of the classical-limit specific heat for all frequencies (Section II). Qualitatively, our model confirms that propagating modes do not contribute significantly to the thermal conductivity of a-SiO2.

The classical-limit mode specific heat is a good approximation for the low-frequency prop-

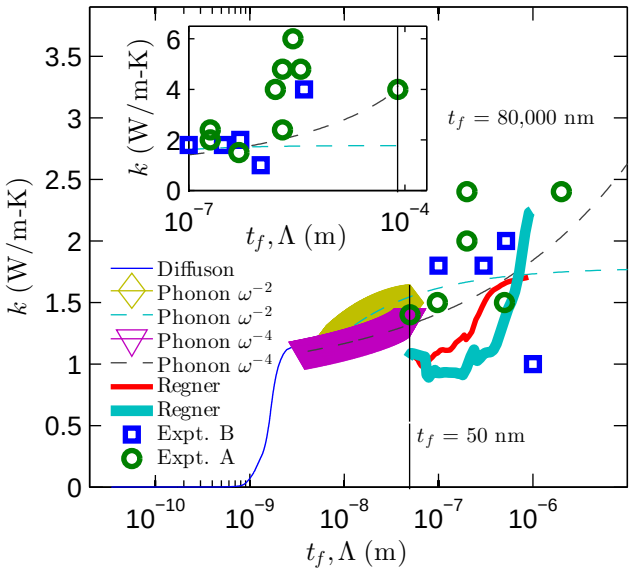

FIG. 8: film thickness dependant thermal conductivity of a-Si from experiment.

agating modes in a-SiO2 and a-Si, which are shown to fully activated by around 10 K.(cite) The classic limit for the mode specific heat is an over-prediction for the high frequency modes in a-SiO2 and a-Si at 300 K.(cite) However, the contribution k_{AF} we predict in the classical limit for mode specific heat for a-Si is nearly the same as the the non-propagating contribution (plateau) predicted by broadband FTDR.(cite) Adjusting the specific heats to include quantum statistical effects... Taking the diffuson contribution k_{AF} to be a constant, which we predict to be $k_{AF} \approx 1$ W/m-K in agreement with other numerical studies(cite) and experiments(cite), we can thus focus on determining the less understood low-frequency propagating contribution k_{ph}.

The scaling of the low-frequency lifetimes in a-Si is not clear from the experimental measurement. For a-Si thin films, varying preparation techniques suggest either quadratic(cite) or quartic(cite) scaling. While there is no clear consensus from various experiments, all predictions in this work demonstrate that the low-frequency modes in bulk a-Si follow a quadratic scaling of the mode lifetimes, which has been observed in previous models of a-Si(cite) and a-SiO2.(cite) Amorphous silicon, however, can be prepared only in thin films,(cite) where voids and other inhomogeneities are unavoidable[89] and can influence the vibrational structure at low frequencies.[17,90] A smooth transition between quadratic and quartic scaling can be achieved using a phenomenological model where a cross-over wavevec-

tor (or frequency) must be specified by experiment.[26] While this cross-over can be identified experimentally for a-SiO2,[23] experiments are limited for a-Si thin films.(cite) Our models are not large enough to investigate the relevant frequency range ($< 110^{12}$ rads/s),(cite) so we considered both quadratic and quartic lifetime scalings when predicting the thermal conductivity accumulation functions in Fig. . Experimental measurements of the cross-over frequency (wavevector) and steepness parameter are needed from experiment to investigate the applicability of this phenomenological model further.(cite) The dependence of a-Si thin film thermal conductivity on thickness,(cite) preparation method,(cite) and hydrogen content(cite) make this particularly challenging. In fact, different experimental studies can be satisfactorily explained using quadratic(cite) or quartic(cite) scalings found that each was a satisfactory explanation for the results found. (cite)

A number of emerging experimental techniques are capable of studying the low-frequency propagating modes in disordered systems. (cite) For amorphous materials, where the propagating contribution k_{ph} is typically smaller than in the crystalline phase, broadband FDTR has demonstrated it can probe the relatively small effect of propagating modes at 300 K. However, the broadband FDTR studies thus far have been limited to one deposition technique and a relatively small range of film thicknesses (500 nm $< t_f <$ 2000 nm).(cite) The nature of the low frequency scaling can be better elucidated using broadband FDTR on films prepared using varying deposition techniques,(cite) a wider-range of film thicknesses (1-100 μm) (cite) and lower-range of temperatures ($10 - 100$ K).(cite) For a-Si, propagating low-frequency have been identified qualitatively by both experimental measurements(cite) and numerical modeling.(cite) It is thus interesting to consider thin films of a-SiGe alloys, which have been demonstrated to have reduced thermal conductivities compared to a-Si.[14] It is not clear what vibrational lifetime scaling at low frequency would be observed in a simple topologically disordered alloy given there is no a consensus for even topologically disordered but chemically ordered systems.(cite) A combination of frequency-domain, time-domain, and variable-physical-heating size measurements would be helpful in investigating.[10,12,20,91]

ENDALAN

This supports the idea of Slack for a-SiO_2[92] While the thermal conductivity of a-SiO , the material is characterized by a constant similar for other amorphous materials such as Lennard-Jones argon[49] and a model of a-GeTe.[47]

That the amorphous phase of Si should have a lower GHz attenuation than many other

amorphous materials is not entirely surprising, as the 2002 review of low-temperature thermal conductivity and internal friction by Pohl, Liu, and Thompson certainly indicates that the fourfold coordinated materials tend to demonstrate weaker anharmonicity.[93]

Theoretical predictions of acoustic attenuation in amor- phous solids generally agree that at room temperature, a quadratic frequency dependence is expected in the frequency range of 10 GHz1 THz and its origins are expected to be the anharmonicity of the interatomic bonds.

Theory from Schirmacher et al. predicted an w4 scaling below a system dependent onset frequency.[94,95]

VI. SUMMARY

BEGINALAN

In this work we investigated the contributions of propagating k_{ph} and non-propagating k_{AF} modes to the total vibrational thermal conductivity k_{vib} of two glasses, a-SiO2 and a-Si. For a-SiO2, the contribution from propagating modes k_{ph} is shown to be negligible compared to k_{vib}. This is confirmed by various experimental measurements, including a broadband FDTR study which probed the vibrational MFPs or a-SiO2. The thermal conductivity accumulation function for our model of a-SiO2 saturates near a MFP of 10 nm, in agreement with the results of Regner et al. who show no systematic variation of the thermal conductivity on L_p,[20] and in agreement with experiments on a-SiO2 thin films which show no systematic variation with film thickness t_f.(cite)

Our model of bulk a-Si has a thermal conductivity k_{vib} with significant contribution from k_{ph}, where the low-frequency propagating modes are best described by a quadratic scaling of the mode lifetimes. The thermal conductivity accumulation predicted for our model of bulk a-Si with a simple boundary scattering model show reasonable agreement with some of the experimentally predicted thermal conductivities using varying film thicknesses and deposition techniques (Fig.).(cite) However, using a quartic scaling with our model also gives a satisfactory agreement with other experimental measurements (Fig.).(cite) These large discrepancies between measured thermal conductivity of various a-Si thin films calls for the need of further experimentation. Broadband techniques,(cite) which have demonstrated the ability to probe a wide-range of vibrational mode frequencies and MFPs, can help

elucidate.(cite)

ENDALAN

[1] D. G. Cahill, W. K. Ford, K. E. Goodson, G. D. Mahan, A. Majumdar, H. J. Maris, R. Merlin, and S. R. Phillpot, Journal of Applied Physics **93**, 793818 (2003).

[2] J.-K. Yu, S. Mitrovic, D. Tham, J. Varghese, and J. R. Heath, Nature Nanotechnology **5**, 718721 (2010).

[3] A. I. Hochbaum, R. Chen, R. D. Delgado, W. Liang, E. C. Garnett, M. Najarian, A. Majumdar, and P. Yang, Nature **451**, 163167 (2008).

[4] G. Pernot, M. Stoffel, I. Savic, F. Pezzoli, P. Chen, G. Savelli, A. Jacquot, J. Schumann, U. Denker, I. Mnch, et al., Nat Mater **9**, 491 (2010), ISSN 1476-1122, URL `http://dx.doi.org/10.1038/nmat2752`.

[5] A. I. Boukai, Y. Bunimovich, J. Tahi-Kheli, J.-K. Yu, W. A. G. Goddard, and J. R. Heath, Nature **451**, 168171 (2008).

[6] B. Poudel, Q. Hao, Y. Ma, Y. Lan, A. Minnich, B. Yu, X. Yan, D. Wang, A. Muto, D. Vashaee, et al., Science **320**, 634638 (2008), URL `http://www.sciencemag.org/content/320/5876/634.abstract`.

[7] A. Ward and D. A. Broido, Phys. Rev. B **81**, 085205 (2010), URL `http://link.aps.org/doi/10.1103/PhysRevB.81.085205`.

[8] M. G. Holland, Physical Review **132**, 2461 (1963).

[9] A. D. Christianson, M. D. Lumsden, O. Delaire, M. B. Stone, D. L. Abernathy, M. A. McGuire, A. S. Sefat, R. Jin, B. C. Sales, D. Mandrus, et al., Phys. Rev. Lett. **101**, 157004 (2008), URL `http://link.aps.org/doi/10.1103/PhysRevLett.101.157004`.

[10] Y. K. Koh and D. G. Cahill, Phys. Rev. B **76**, 075207 (2007), URL `http://link.aps.org/doi/10.1103/PhysRevB.76.075207`.

[11] M. Highland, B. C. Gundrum, Y. K. Koh, R. S. Averback, D. G. Cahill, V. C. Elarde, J. J. Coleman, D. A. Walko, and E. C. Landahl, Phys. Rev. B **76**, 075337 (2007), URL `http://link.aps.org/doi/10.1103/PhysRevB.76.075337`.

[12] A. J. Minnich, J. A. Johnson, A. J. Schmidt, K. Esfarjani, M. S. Dresselhaus, K. A. Nelson, and G. Chen, Phys. Rev. Lett. **107**, 095901 (2011), URL `http://link.aps.org/doi/10.1103/PhysRevLett.107.095901`.

[13] F. Yang and C. Dames, Physical Review B **87**, 035437 (2013), URL `http://link.aps.org/`

doi/10.1103/PhysRevB.87.035437.

[14] J. L. Feldman, M. D. Kluge, P. B. Allen, and F. Wooten, Physical Review B **48**, 1258912602 (1993).

[15] D. G. Cahill, M. Katiyar, and J. R. Abelson, Physical Review B **50**, 60776081 (1994).

[16] J. L. Feldman, P. B. Allen, and S. R. Bickham, Phys. Rev. B **59**, 35513559 (1999), URL http://link.aps.org/doi/10.1103/PhysRevB.59.3551.

[17] X. Liu, J. L. Feldman, D. G. Cahill, R. S. Crandall, N. Bernstein, D. M. Photiadis, M. J. Mehl, and D. A. Papaconstantopoulos, Phys. Rev. Lett. **102**, 035901 (2009), URL http://link.aps.org/doi/10.1103/PhysRevLett.102.035901.

[18] H.-S. Yang, D. G. Cahill, X. Liu, J. L. Feldman, R. S. Crandall, B. A. Sperling, and J. R. Abelson, Phys. Rev. B **81**, 104203 (2010), URL http://link.aps.org/doi/10.1103/PhysRevB.81.104203.

[19] Y. He, D. Donadio, J.-H. Lee, J. C. Grossman, and G. Galli, ACS Nano **5**, 1839\textbackslashtextbackslashtextbackslashtextbackslashtextbackslash961844 (2011).

[20] K. T. Regner, D. P. Sellan, Z. Su, C. H. Amon, A. J. McGaughey, and J. A. Malen, Nat Commun **4**, 1640 (2013), URL http://dx.doi.org/10.1038/ncomms2630.

[21] S.-M. Lee and D. G. Cahill, Journal of Applied Physics **81**, 25902595 (1997).

[22] T. Yamane, N. Nagai, S.-i. Katayama, and M. Todoki, Journal of Applied Physics **91**, 97729776 (2002), URL http://link.aip.org/link/?JAP/91/9772/1.

[23] C. Masciovecchio, G. Baldi, S. Caponi, L. Comez, S. Di Fonzo, D. Fioretto, A. Fontana, A. Gessini, S. C. Santucci, F. Sette, et al., Phys. Rev. Lett. **97**, 035501 (2006), URL http://link.aps.org/doi/10.1103/PhysRevLett.97.035501.

[24] G. Baldi, V. M. Giordano, G. Monaco, F. Sette, E. Fabiani, A. Fontana, and G. Ruocco, Phys. Rev. B **77**, 214309 (2008), URL http://link.aps.org/doi/10.1103/PhysRevB.77.214309.

[25] G. Baldi, V. M. Giordano, G. Monaco, and B. Ruta, Phys. Rev. Lett. **104**, 195501 (2010), URL http://link.aps.org/doi/10.1103/PhysRevLett.104.195501.

[26] G. Baldi, V. M. Giordano, and G. Monaco, Phys. Rev. B **83**, 174203 (2011), URL http://link.aps.org/doi/10.1103/PhysRevB.83.174203.

[27] G. Baldi, M. Zanatta, E. Gilioli, V. Milman, K. Refson, B. Wehinger, B. Winkler, A. Fontana, and G. Monaco, Phys. Rev. Lett. **110**, 185503 (2013), URL http://link.aps.org/doi/10.1103/PhysRevLett.110.185503.

[28] L. Wieczorek, H. Goldsmid, and G. Paul, in *Thermal Conductivity 20*, edited by D. Hasselman and J. Thomas, J.R. (Springer US, 1989), pp. 235–241, ISBN 978-1-4612-8069-9, URL http://dx.doi.org/10.1007/978-1-4613-0761-7_22.

[29] H. Wada and T. Kamijoh, Japanese Journal of Applied Physics **35**, L648L650 (1996), URL http://jjap.jsap.jp/link?JJAP/35/L648/.

[30] B. L. Zink, R. Pietri, and F. Hellman, Physical Review Letters **96**, 055902 (2006), URL http://link.aps.org/doi/10.1103/PhysRevLett.96.055902.

[31] B. S. W. Kuo, J. C. M. Li, and A. W. Schmid, Applied Physics A: Materials Science & Processing **55**, 289296 (1992), ISSN 0947-8396, 10.1007/BF00348399, URL http://dx.doi.org/10.1007/BF00348399.

[32] S. Moon, M. Hatano, M. Lee, and C. P. Grigoropoulos, International Journal of Heat and Mass Transfer **45**, 2439 2447 (2002), ISSN 0017-9310, URL http://www.sciencedirect.com/science/article/pii/S0017931001003477.

[33] G. Pompe and E. Hegenbarth, physica status solidi (b) **147**, 103 (1988), ISSN 1521-3951, URL http://dx.doi.org/10.1002/pssb.2221470109.

[34] D. G. Cahill, H. E. Fischer, T. Klitsner, E. T. Swartz, and R. O. Pohl, Journal of Vaccuum Science and Technology A **7**, 12591266 (1989).

[35] B. L. Zink, R. Islam, D. J. Smith, and F. Hellman, Phys. Rev. B **74**, 205209 (2006), URL http://link.aps.org/doi/10.1103/PhysRevB.74.205209.

[36] N. W. Ashcroft and N. D. Mermin, *Solid State Physics* (Saunders, Fort Worth, 1976).

[37] M. T. Dove, *Introduction to Lattice Dynamics* (Cambridge, Cambridge, 1993).

[38] J. M. Ziman, *Electrons and Phonons* (Oxford, New York, 2001).

[39] A. J. H. McGaughey and M. Kaviany, International Journal of Heat and Mass Transfer **47**, 17831798 (2004).

[40] Y. He, D. Donadio, and G. Galli, Applied Physics Letters **98**, 144101 (2011), URL http://link.aip.org/link/?APL/98/144101/1.

[41] D. Donadio and G. Galli, Phys. Rev. Lett. **102**, 195901 (2009).

[42] J. K. Flicker and P. L. Leath, Phys. Rev. B **7**, 22962305 (1973), URL http://link.aps.org/doi/10.1103/PhysRevB.7.2296.

[43] P. B. Allen and J. L. Feldman, Physical Review B **48**, 1258112588 (1993).

[44] A. Alam and A. Mookerjee, Phys. Rev. B **72**, 214207 (2005), URL http://link.aps.org/doi/

10.1103/PhysRevB.72.214207.

[45] P. G. Klemens, Proceedings of the Physical Society. Section A **68** (1955).

[46] D. A. McQuarrie, *Statistical Mechanics* (University Science Books, Sausalito, 2000).

[47] G. C. Sosso, D. Donadio, S. Caravati, J. Behler, and M. Bernasconi, Phys. Rev. B **86**, 104301 (2012), URL http://link.aps.org/doi/10.1103/PhysRevB.86.104301.

[48] P. B. Allen and J. Kelner, American Journal of Physics **66**, 497506 (1998).

[49] J. Larkin and A. McGaughey, Journal of Applied Physics (2013).

[50] D. Cahill and R. Pohl, Annual Review of Physical Chemistry **39**, 93121 (1988).

[51] D. G. Cahill, S. K. Watson, and R. O. Pohl, Phys. Rev. B **46**, 61316140 (1992), URL http://link.aps.org/doi/10.1103/PhysRevB.46.6131.

[52] G. T. Barkema and N. Mousseau, Phys. Rev. B **62**, 49854990 (2000), URL http://link.aps.org/doi/10.1103/PhysRevB.62.4985.

[53] M. Durandurdu and D. A. Drabold, Phys. Rev. B **66**, 155205 (2002), URL http://link.aps.org/doi/10.1103/PhysRevB.66.155205.

[54] N. Bernstein, J. L. Feldman, and M. Fornari, Phys. Rev. B **74**, 205202 (2006), URL http://link.aps.org/doi/10.1103/PhysRevB.74.205202.

[55] S. Plimpton, Journal of Computational Physics **117**, 1 19 (1995), ISSN 0021-9991, URL http://www.sciencedirect.com/science/article/pii/S002199918571039X.

[56] J. D. Gale and A. L. Rohl, Molecular Simulation **29**, 291 (2003).

[57] M. L. Williams and H. J. Maris, Phys. Rev. B **31**, 45084515 (1985), URL http://link.aps.org/doi/10.1103/PhysRevB.31.4508.

[58] Y. M. Beltukov, V. I. Kozub, and D. A. Parshin, Phys. Rev. B **87**, 134203 (2013), URL http://link.aps.org/doi/10.1103/PhysRevB.87.134203.

[59] S. N. Taraskin and S. R. Elliott, EPL (Europhysics Letters) **39**, 37 (1997), URL http://stacks.iop.org/0295-5075/39/i=1/a=037.

[60] J. Horbach, W. Kob, and K. Binder, The European Physical Journal B - Condensed Matter and Complex Systems **19**, 531 (2001), ISSN 1434-6028, URL http://dx.doi.org/10.1007/s100510170299.

[61] W. Gtze and M. R. Mayr, Phys. Rev. E **61**, 587606 (2000), URL http://link.aps.org/doi/10.1103/PhysRevE.61.587.

[62] V. Vitelli, N. Xu, M. Wyart, A. J. Liu, and S. R. Nagel, Phys. Rev. E **81**, 021301 (2010), URL

http://link.aps.org/doi/10.1103/PhysRevE.81.021301.

[63] T. Hori, T. Shiga, and J. Shiomi, Journal of Applied Physics **113**, 203514 (2013), URL http://link.aip.org/link/?JAP/113/203514/1.

[64] J. C. Duda, T. S. English, D. A. Jordan, P. M. Norris, and W. A. Soffa, Journal of Physics: Condensed Matter **23**, 205401 (2011), URL http://stacks.iop.org/0953-8984/23/i=20/a=205401.

[65] P. B. Allen, J. L. Feldman, J. Fabian, and F. Wooten, Philosophical Magazine B **79**, 17151731 (1999).

[66] N. L. Green, D. Kaya, C. E. Maloney, and M. F. Islam, Physical Review E **83**, 051404 (2011), URL http://link.aps.org/doi/10.1103/PhysRevE.83.051404.

[67] S. Volz and G. Chen, Physical Review B **61**, 26512656 (2000).

[68] J. L. Feldman, Journal of Non-Crystalline Solids **307310**, 128 (2002), ISSN 0022-3093, URL http://www.sciencedirect.com/science/article/pii/S0022309302014503.

[69] R. Biswas, A. M. Bouchard, W. A. Kamitakahara, G. S. Grest, and C. M. Soukoulis, Phys. Rev. Lett. **60**, 22802283 (1988), URL http://link.aps.org/doi/10.1103/PhysRevLett.60.2280.

[70] L. E. Silbert, A. J. Liu, and S. R. Nagel, Phys. Rev. E **79**, 021308 (2009), URL http://link.aps.org/doi/10.1103/PhysRevE.79.021308.

[71] B. Ruzicka, T. Scopigno, S. Caponi, A. Fontana, O. Pilla, P. Giura, G. Monaco, E. Pontecorvo, G. Ruocco, and F. Sette, Phys. Rev. B **69**, 100201 (2004), URL http://link.aps.org/doi/10.1103/PhysRevB.69.100201.

[72] A. J. C. Ladd, B. Moran, and W. G. Hoover, Physical Review B **34**, 50585064 (1986).

[73] A. J. H. McGaughey and M. Kaviany, Physical Review B **69**, 094303 (2004).

[74] J. E. Turney, E. S. Landry, A. J. H. McGaughey, and C. H. Amon, Phys. Rev. B **79**, 064301 (2009), URL http://link.aps.org/doi/10.1103/PhysRevB.79.064301.

[75] J. M. Larkin, J. E. Turney, A. D. Massicotte, C. H. Amon, and A. J. H. McGaughey, to appear in Journal of Computational and Theoretical Nanoscience (2012).

[76] V. Martin-Mayor, M. Mezard, G. Parisi, and P. Verrocchio, The Journal of Chemical Physics **114**, 8068 (2001), URL http://link.aip.org/link/?JCP/114/8068/1.

[77] P. Sheng and M. Zhou, Science **253**, 539542 (1991), URL http://www.sciencemag.org/content/253/5019/539.abstract.

[78] V. Mazzacurati, G. Ruocco, and M. Sampoli, EPL (Europhysics Letters) **34**, 681 (1996), URL

http://stacks.iop.org/0295-5075/34/i=9/a=681.

[79] J. Fabian and P. B. Allen, Phys. Rev. Lett. **77**, 38393842 (1996), URL http://link.aps.org/doi/10.1103/PhysRevLett.77.3839.

[80] J. Fabian, J. L. Feldman, C. S. Hellberg, and S. M. Nakhmanson, Phys. Rev. B **67**, 224302 (2003), URL http://link.aps.org/doi/10.1103/PhysRevB.67.224302.

[81] S. R. Bickham, Phys. Rev. B **59**, 48944897 (1999), URL http://link.aps.org/doi/10.1103/PhysRevB.59.4894.

[82] S. R. Bickham and J. L. Feldman, Phys. Rev. B **57**, 1223412238 (1998), URL http://link.aps.org/doi/10.1103/PhysRevB.57.12234.

[83] J. T. Edwards and D. J. Thouless, Journal of Physics C: Solid State Physics **5**, 807 (1972), URL http://stacks.iop.org/0022-3719/5/i=8/a=007.

[84] W. Garber, F. M. Tangerman, P. B. Allen, and J. L. Feldman, Philosophical Magazine Letters **81**, 433439 (2001), URL http://www.tandfonline.com/doi/abs/10.1080/09500830110041666.

[85] N. Xu, V. Vitelli, M. Wyart, A. J. Liu, and S. R. Nagel, Phys. Rev. Lett. **102**, 038001 (2009), URL http://link.aps.org/doi/10.1103/PhysRevLett.102.038001.

[86] G. Ruocco, F. Sette, R. Di Leonardo, G. Monaco, M. Sampoli, T. Scopigno, and G. Viliani, Phys. Rev. Lett. **84**, 57885791 (2000), URL http://link.aps.org/doi/10.1103/PhysRevLett.84.5788.

[87] Y. H. Lee, R. Biswas, C. M. Soukoulis, C. Z. Wang, C. T. Chan, and K. M. Ho, Phys. Rev. B **43**, 65736580 (1991), URL http://link.aps.org/doi/10.1103/PhysRevB.43.6573.

[88] M. S. Love and A. C. Anderson, Phys. Rev. B **42**, 18451847 (1990), URL http://link.aps.org/doi/10.1103/PhysRevB.42.1845.

[89] S. Li, Y. Jiang, Z. Wu, J. Wu, Z. Ying, Z. Wang, W. Li, and G. J. Salamo, Applied Surface Science **257**, 8326 (2011), ISSN 0169-4332, URL http://www.sciencedirect.com/science/article/pii/S0169433211004715.

[90] J. L. Feldman, N. Bernstein, D. A. Papaconstantopoulos, and M. J. Mehl, Phys. Rev. B **70**, 165201 (2004), URL http://link.aps.org/doi/10.1103/PhysRevB.70.165201.

[91] M. E. Siemens, Q. Li, R. Yang, K. A. Nelson, E. H. Anderson, M. M. Murnane, and H. C. Kapteyn, Nature Materials **9**, 2630 (2010).

[92] G. A. Slack (Academic Press, 1979), vol. 34 of *Solid State Physics*, p. 1 71, URL http:

//www.sciencedirect.com/science/article/pii/S0081194708603598.

[93] R. O. Pohl, X. Liu, and E. Thompson, Rev. Mod. Phys. **74**, 9911013 (2002), URL http://link.aps.org/doi/10.1103/RevModPhys.74.991.

[94] W. Schirmacher, EPL (Europhysics Letters) **73**, 892 (2006), URL http://stacks.iop.org/0295-5075/73/i=6/a=892.

[95] W. Schirmacher, G. Ruocco, and T. Scopigno, Phys. Rev. Lett. **98**, 025501 (2007), URL http://link.aps.org/doi/10.1103/PhysRevLett.98.025501.